ELSEVIER

NeuroImage

www.elsevier.com/locate/ynimg
NeuroImage 33 (2006) 27–38

White and gray matter development in human fetal, newborn and pediatric brains

Hao Huang,[a] Jiangyang Zhang,[a] Setsu Wakana,[a,b] Weihong Zhang,[a,b] Tianbo Ren,[c] Linda J. Richards,[d] Paul Yarowsky,[e] Pamela Donohue,[f] Ernest Graham,[g] Peter C.M. van Zijl,[a,b] and Susumu Mori,[a,b,*]

[a]*Department of Radiology, Johns Hopkins University School of Medicine 720 Rutland Avenue, Baltimore, MD 21205, USA*
[b]*F.M. Kirby Center for Functional Magnetic Resonance Imaging, Kennedy Krieger Institute, 707 North Broadway, Baltimore, MD 21205, USA*
[c]*Department of Anatomy and Neurobiology, University of Maryland, 655 West Baltimore Street, Baltimore, MD 21201, USA*
[d]*Department of Anatomy and Developmental Biology, The University of Queensland, St Lucia, Queensland, 4072, Australia*
[e]*Department of Pharmacology and Experimental Therapeutics, University of Maryland, 655 West Baltimore Street, Baltimore, MD 21201, USA*
[f]*Department of Pediatrics, Johns Hopkins University School of Medicine 720 Rutland Avenue, Baltimore, MD 21205, USA*
[g]*Department of Gynecology and Obstetrics, Johns Hopkins University School of Medicine 720 Rutland Avenue, Baltimore, MD 21205, USA*

Received 29 March 2006; revised 29 May 2006; accepted 6 June 2006
Available online 14 August 2006

Brain anatomy is characterized by dramatic growth from the end of the second trimester through the neonatal stage. The characterization of normal axonal growth of the white matter tracts has not been well-documented to date and could provide important clues to understanding the extensive inhomogeneity of white matter injuries in cerebral palsy (CP) patients. However, anatomical studies of human brain development during this period are surprisingly scarce and histology-based atlases have become available only recently. Diffusion tensor magnetic resonance imaging (DTMRI) can reveal detailed anatomy of white matter. We acquired diffusion tensor images (DTI) of postmortem fetal brain samples and *in vivo* neonates and children. Neural structures were annotated in two-dimensional (2D) slices, segmented, measured, and reconstructed three-dimensionally (3D). The growth status of various white matter tracts was evaluated on cross-sections at 19–20 gestational weeks, and compared with 0-month-old neonates and 5- to 6-year-old children. Limbic, commissural, association, and projection white matter tracts and gray matter structures were illustrated in 3D and quantitatively characterized to assess their dynamic changes. The overall pattern of the time courses for the development of different white matter is that limbic fibers develop first and association fibers last and commissural and projection fibers are forming from anterior to posterior part of the brain. The resultant DTMRI-based 3D human brain data will be a valuable resource for human brain developmental study and will provide reference standards for diagnostic radiology of premature newborns.

Keywords: DTI; Brain development; Atlas; Neonate; PVL

Introduction

It has been shown that diffusion tensor magnetic resonance imaging (DTMRI) can reveal the detailed anatomy of human brain white matter (Basser et al., 1994; Pierpaoli and Basser, 1996; Makris et al., 1997; Stieltjes et al., 2001; Catani et al., 2002; Wakana et al., 2004, Mori et al., 2005). The contrast, which is based on structural alignment, provides unique information about axonal tracts and is difficult to obtain by any other non-invasive technique. This information is especially useful to delineate the anatomy of premature brain that is not myelinated and for which relaxation-based contrast is inadequate (Huppi et al., 1998; Neil et al., 1998; Mori et al., 2001; McKinstry et al., 2002; Mukherjee et al., 2002; Maas et al., 2004; Partridge et al., 2004; Schneider et al., 2004; Hermoye et al., 2006). The technique can delineate injuries in specific white matter tracts as well as demonstrate the rearrangement of tracts (Huppi and Inderc, 2001; Hoon et al., 2002; Miller et al., 2002; Lee et al., 2005; Thomas et al., 2005). As DTI becomes widely available in clinical scanners, it is likely that DTI will be an important diagnostic tool in this field in the future.

Among pediatric cases, imaging of pre- or full-term infants for clinical indications is of great interest. Routinely used diagnostic methods, such as electronic monitoring and ultrasound, often have poor sensitivity to significant abnormalities in neonate brains. A new imaging modality that can precisely delineate anatomical and physiological abnormalities is urgently needed. Furthermore, it has been demonstrated that various injuries, due to perinatal risks, often lead to damage in selective white matter. Precise delineation of the status of specific white matter tracts may provide more accurate diagnosis. Because of the advances in the critical care of pre-term infants, the survival rate of premature infants has increased dramatically in recent years. Identification of abnormalities in the early phase of injuries, identification of perinatal risk

Abbreviations: CP, cerebral palsy; DT, diffusion tensor; MRI, magnetic resonance imaging; 2D/3D, two/three dimensional.

* Corresponding author. Johns Hopkins University School of Medicine, Department of Radiology, 217 Traylor Building, 720 Rutland Avenue, Baltimore, MD 21205, USA. Fax: +1 410 614 1948.
E-mail address: Susumu@mri.jhu.edu (S. Mori).

Available online on ScienceDirect (www.sciencedirect.com).

1053-8119/$ - see front matter © 2006 Elsevier Inc. All rights reserved.
doi:10.1016/j.neuroimage.2006.06.009

factors, and understanding of injury development are becoming more important than ever.

The primary purpose of this study is to characterize normal neuroanatomy at the end of the second trimester and neonatal stage, especially the white matter anatomy. Histology-based atlases of the developing human brain are surprisingly scarce, and comprehensive atlases of second- and third-trimester development have only recently become available (Bayer and Altman, 2004, 2005). At the end of the second trimester, early-developed white matter tracts, such as the thalamo-cortical fibers, are known to have already formed. However, there are many white matter tracts that are still rapidly growing at this time. The time courses of axonal growth of these white matter tracts have not been well-documented as yet and could provide important clues to the understanding of the extensive inhomogeneity of white matter injuries in cerebral palsy (CP) patients.

In this study, limbic, commissural, association, and projection white matter tracts and gray matter structures were illustrated in 3D and quantitatively characterized to assess their dynamic changes. We explored the potential of DTMRI to trace the time courses of development of different white matter tracts. The overall pattern of white matter development is that limbic fibers develop first and association fibers last and commissural and projection fibers are forming from anterior to posterior part of the brain. Three distinct time points were chosen to study developing neuroanatomy with DTI. First, we used postmortem specimens of fetal brains at 19–20 weeks of gestational age. Using ample imaging time (up to 24 h), these data provide high-resolution, high-quality MRI to elucidate brain anatomy and to investigate MRI/DTI contrasts. This developmental stage is a few weeks earlier than the possible survival of infants (22–24 gestational weeks). The second time point is full-term, in which we imaged healthy volunteers while asleep. These images can be considered a normal reference for the full-term infant. The third time point is 5–6 years old. Around this age, pediatric brains seem to mature to the point where MR images look very similar to those of an adult brain. We expect that these data will help in the understanding of the contrasts on DTI images from premature infants and in the detection of anatomical abnormalities.

Materials and methods

Postmortem specimen

Samples

Postmortem samples of 19–20 gestational week fetal brains ($n=3$) were borrowed from the University of Maryland Tissue Bank. The samples were fixed with 4% paraformaldehyde in phosphate-buffered saline (PBS) and kept immersed in the fixation solution until 48 h before the MR experiments. The samples were then put into PBS to wash out the fixative and replace the fixation solution inside the tissue. The samples were bathed with PBS throughout the MR scanning. Unfortunately, it is very difficult to obtain fetal brains without damage. The most common damages included a severed corpus callosum (19 gestational week sample) and a damaged brainstem (20 gestational week sample). To demonstrate the most intact anatomy, we used the 19 gestational week sample for the brainstem and the 20 gestational week sample for the cerebral hemispheres in the slice-by-slice anatomical annotation.

Imaging parameters

Three-dimensional (3D) spin echo diffusion tensor imaging and T_1-weighted images were acquired in a 4.7 T Bruker scanner. The fetal brains bathed in PBS were placed in custom-made chambers during the scan. A 70 mm (inner diameter) volume coil was used for RF transmission and reception. For DTI imaging, a 3D multiple spin echo diffusion tensor sequence was used. Multiple echoes (number of echoes = 8) were adopted to improve the signal to noise ratio (SNR). A set of diffusion-weighted images (DWI) was acquired in 7 linearly independent directions. DWI parameters for the 4.7 T scanner were: TE = 32.5 ms; TR = 0.7 s; Field of View (FOV) = 48 mm/44 mm/44 mm (19 gestational week) or 54 mm/53 mm/37 mm (20 gestational week); and imaging matrix = 128 × 72 × 72 (zero-filled to data matrix = 128 × 128 × 128). Co-registered T_1-weighted images with the same FOV were also acquired with the fast spin echo sequence. T_1-weighted imaging parameters were: effective TE = 27 ms; TR = 0.3 s; and imaging matrix = 256 × 160 × 160 (zero-filled to data matrix = 256 × 256 × 256). The total DTI scanning times were 21 h with three signal averages. The total T_1-weighted image scanning time was 2 h with six signal averages.

Term infant and pediatric studies

Subjects

For the 0-month-old newborn babies ($F=3$) and the 5- to 6-year-old pediatric subjects ($F=1$, $M=2$), permission was obtained from the Johns Hopkins Hospital's Institutional Review Board and written informed consent was provided by the subjects' parents. The healthy volunteers for the pediatric cases did not have any prior neurological conditions. The average (standard deviations) body weight and head circumference of the neonates were 3346.7 (±248.5) kg and 33.9 (±0.52) cm, and their gestational ages were 39–40 weeks. APGAR scores were $9_1\ 9_5$, $6_1\ 8_5$, and $2_1\ 7_5\ 9_{10}$.

Imaging parameters

Images were acquired using a SENSE head coil on a 1.5 T whole-body MR scanner (Philips Medical Systems, Best, The Netherlands) equipped with explorer gradients (40 mT/m). For DTI acquisitions, a single-shot, spin echo, echo planar sequence (SE-EPI) was used, with diffusion gradients applied in 30 non-collinear directions (Jones et al., 1999) and $b=700$ s/mm^2. Five additional reference images with the least diffusion weighting ($b=33$ s/mm^2) were also acquired. Forty to fifty axial slices were acquired, parallel to the AC–PC line. The FOV, the size of the acquisition matrix, and the slice thickness were 150 × 150 mm/80 × 80/1.88 mm for the neonate and 220 × 220 mm/96 × 96/2.3 mm for the pediatric subject. All images were zero-filled to the final reconstruction matrix of 256 × 256. Other imaging parameters were: TR = 7859 ms; TE = 80 ms; diffusion b-value = 700 s/mm^2; and SENSE reduction factor = 2.5. To improve the signal to noise ratio, two datasets were acquired, leading to a total acquisition time of approximately 10 min. No cardiac gating was used.

Image analysis

Postprocessing and visualization of DTI

The diffusion-weighted images were transferred to an off-line PC workstation and processed by DtiStudio (Hangyi Jiang, and Susumu Mori, Johns Hopkins University, Kennedy Krieger Institute, lbam.med.jhmi.edu). Six elements of the diffusion tensor were determined by multivariate least-square fitting. The tensor was diagonalized to obtain three eigenvalues (λ_{1-3}) and eigenvectors (v_{1-3}). Anisotropy was measured by calculating fractional anisotropy (FA) 2.

The eigenvector associated with the largest eigenvalue (v_1) was used as an indicator of fiber orientation. For color-coded orientation maps, red (R), green (G), and blue (B) colors were assigned to left–right, anterior–posterior, and superior–inferior orientations, respectively. For the color presentation, 24-bit color was used, in which each RGB color had 8-bit (0–255) intensity levels. The unit vector $v_1(=\lfloor v_{1x}, v_{1y}, v_{1z} \rfloor)$ always fulfills the condition, $v_{1x}^2+v_{1y}^2+v_{1z}^2=1$. Intensity values of v_{1x}^2*255, v_{1y}^2*255, and v_{1z}^2*255 were assigned to the R(ed), G(reen), and B(lue) channel, respectively. In order to suppress orientation information in isotropic brain regions, the 24-bit color value was multiplied by FA, which was scaled from 0 to 1. Apparent diffusion coefficient (ADC) was calculated as 1/3 of the trace of the diffusion tensor. Average diffusion-weighted images were obtained by adding all diffusion-weighted images.

Structure assignment and reconstruction

Gray matter. Various gray matter structures were assigned using averaged diffusion-weighted images, color-coded orientation maps, and the Bayer and Altman's fetal brain atlas as guidance (Bayer and Altman, 2004, 2005). The assigned gray matter structures were manually segmented using software Amira (TGS, San Diego, CA). The following major gray matter structures were identified, segmented, and reconstructed: the thalamus; the ganglionic eminence; the putamen; the globus pallidus; the caudate; the hippocampus; and the cortex.

White matter tracts. Various white matter tracts were identified based on color-coded orientation maps. White matter tracts were identified and assigned when they were found in all samples reproducibly and agree with the Bayer and Altman's atlases (Bayer and Altman, 2004, 2005). For visual assistance, identified white matter tracts were three-dimensionally reconstructed using the fiber assignment by a continuous tracking method (FACT, Mori et al., 1999; Xue et al., 1999). For the reconstruction, a fractional anisotropy threshold of 0.15 and an inner product threshold of 0.75 were used.

Results

Comparison of imaging contrasts

Fig. 1 shows comparison of different MRI contrasts from a postmortem fetal sample at 19 gestational weeks of age. The images are coronal images at the paracentral lobule. Four of them (aDWI: averaged diffusion-weighted image, FA: fractional anisotropy map, Color: color-coded orientation map, and ADC: averaged diffusion constant map) are derived from DTI. Fig. 1e shows conventional T_1-weighted images. The relaxation-based image (Fig. 1e) excels in delineating overall brain shape, several cortical layers, and the ganglionic eminence (GE), a transient structure for basal ganglion. However, because of lack of myelination, gray matter–white matter differentiation is not clear. For example, the boundary of the internal capsule (ic) and the thalamus (Tha) is not well-appreciated.

DTI-based contrasts provide very different information from T_1-weighted images. As expected, white matter tracts have high intensity in the FA, and color-coded maps. For example, the location of the cingulum bundle (cg) and the internal capsule can be appreciated only in the FA and color maps. An advantage of conventional T_1-weighted images is that they achieve higher image resolution than DTI. This point is evident in the hippocampus where layer structures are clearly visible in the T_1-weighted image (Fig. 1e). However, for other regions where T_1-weighted image lacks contrasts, the higher resolution does not necessarily provide more

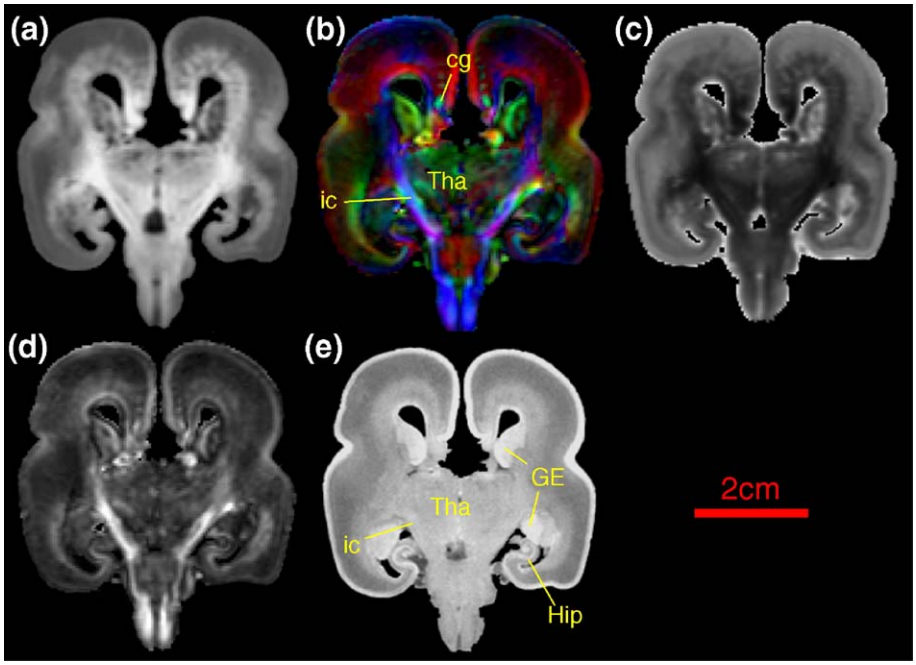

Fig. 1. Comparison of different image contrasts from a 19 gestational week fetal brain. (a) Average diffusion-weighted image, (b) color-coded orientation map, (c) ADC map, (d) FA map, and (e) T_1-weighted image. In the color maps, the red, green, and blue colors represent fibers running along the right–left, anterior–posterior, and superior–inferior orientations. Abbreviations: cg: cingulum; ic: internal capsule; GE: ganglionic eminence; Hip: hippocampus; Tha: thalamus.

anatomical information. Relaxation-based contrasts and DTI, thus, seem to provide complementary information.

3D volume reconstruction

With the high contrasts provided by DTI, multiple neural structures can be identified and segmented. Fig. 2 shows 3D reconstruction of major anatomical structures at the three development stages. The first column shows the 3D reconstruction of the whole brain (gray); the second column shows brainstem (blue) and cerebellum (brown); the third column shows the ventricle (cyan), putamen, and globus pallidus (green) and caudate nucleus (red); the fourth column shows the hippocampus (pink); and the fifth column shows the thalamus (yellow) and the ganglionic eminence (orange). At 19–20 gestational weeks, the brain has a relatively smooth surface. The sylvian fissure is the only apparent sulcus in this view, and the temporal lobe is already visible. The cerebellum is not well developed and a large portion of the cerebral hemisphere is occupied by the ventricle. The basal ganglia and hippocampus can be clearly identified at this early stage.

Table 1 and Fig. 3 give the volumes of the brains of 19–20 gestational week fetuses, newborn babies, and 5- to 6-year-old children. For the data in Table 1, each time point represents the volume measurement of 3 different brains. The mean and standard deviation (SD) of the absolute volume and its relative proportion in relation to the whole brain volume are also listed in Table 1. From 19 to 20 gestational week fetal brains to term (approximately 40 weeks), the whole brain volume increases almost 17 times, while the increase is about 3 to 4 times from term to 5–6 years old. The brain structures develop disproportionately during these periods. From 19 gestational weeks to term, the brain growth is characterized by a rapid decrease in the relative size of the ventricle and the brainstem, while from term to a 5- to 6-year-old child, the relative proportion of the cerebellum increases.

Slice-by-slice atlas

A slice-by-slice comparison of the 19–20 gestational week fetal brain, newborn brain, and 5- to 6-year pediatric brain is shown in Figs. 4a to d. Compared to newborn babies and 5- to 6-year-old children, the relative sizes of cerebellar peduncles and medial lemnisci are smaller in the fetal brain, while the descending tracts (cst) are dominant. Smaller relative sizes of the cerebellar peduncles are consistent with the smaller relative size of the cerebellum.

Decussation of the superior cerebellar peduncle is already formed at 19 gestational weeks (Fig. 4b). The sagittal stratum and the external capsule (which contains association tracts, such as the inferior longitudinal fasciculus and inferior fronto-occipital fasciculus) cannot be well-appreciated in the fetus. On axial slices of the midbrain levels (Fig. 4b), it can be seen that the cerebral peduncle, anterior commissure, and limbic fibers (cingulum and stria terminalis/fornix) are well-formed. The optic tract and the optic radiation

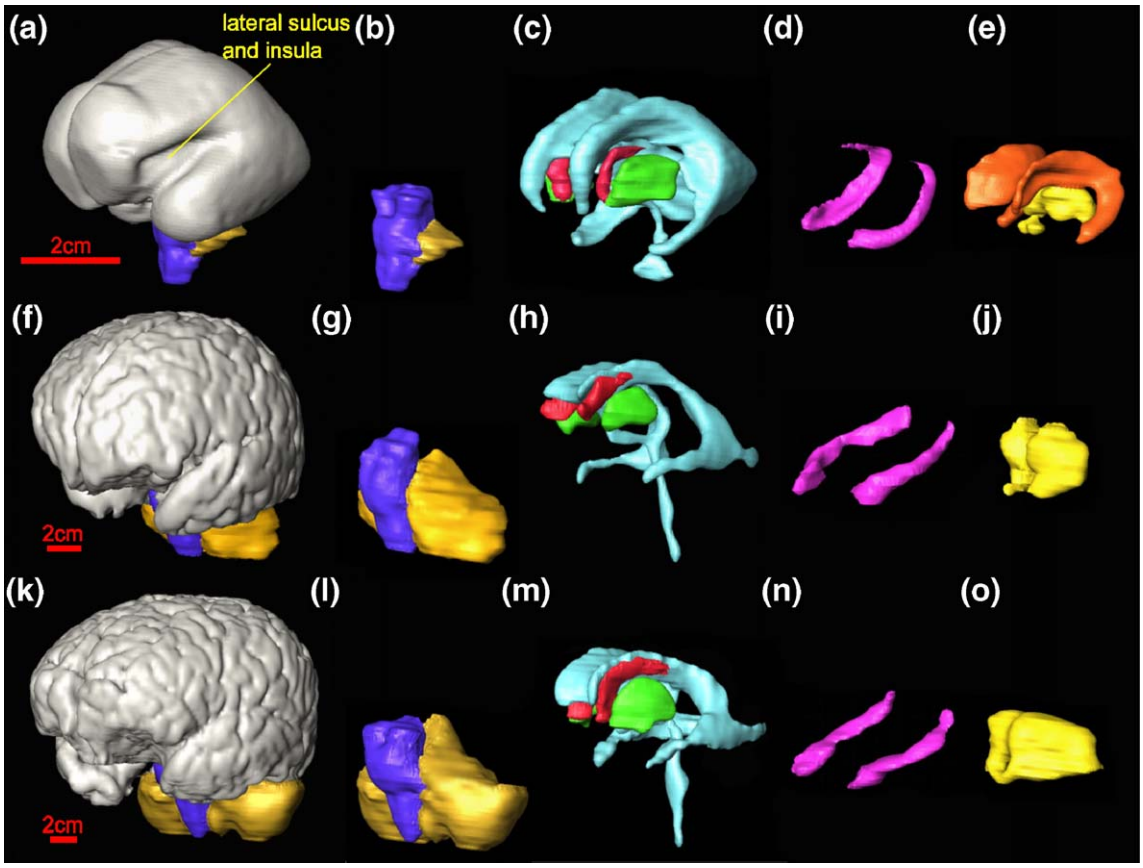

Fig. 2. 3D reconstruction of the cortex (a, f, k), brain stem, and cerebellum (b, g, l), ventricle, caudate nucleus, basal ganglia (c, h, m), hippocampus (d, i, n), thalamus, and ganglionic eminence (e, j, o) of a 19 gestational week fetal brain (a–e), newborn baby brain (f–j), and 5-year-old pediatric brain (k–o). Color-coding: gray: cerebrum; blue: brain stem; brown: cerebellum; cyan: ventricle; green: putamen and globus pallidus; red: caudate nucleus; pink: hippocampus; yellow: thalamus; and orange: ganglionic eminence.

Table 1
Absolute volumes and relative sizes of neural structures at different ages

Subjects/Neural structures	Whole brain (mean±SD)	Cerebrum (mean±SD)	Cerebellum (mean±SD)	Brain stem (mean±SD)	Ventricle (mean±SD)
19 gestational week fetus (ml)	22.27±0.80	18.67±1.00	0.59±0.04	0.93±0.03	2.07±0.21
Newborn baby (ml)	367.3±15.7	331.6±15.8	24.4±0.5	4.8±0.2	6.5±0.4
5/6-year child (ml)	1257.7±85.6	1096.2±74.4	122.8±4.8	20.5±1.6	18.2±3.4
19-week fetus (%)	100±3.6	83.8±4.5	2.7±0.2	4.2±0.1	9.3±0.9
Newborn baby (%)	100±4.3	90.3±4.3	6.6±0.1	1.3±0.1	1.8±0.1
5/6-year child (%)	100±6.8	87.2±5.9	9.8±0.4	1.6±0.1	1.4±0.3

can be identified, which are connected to the lateral geniculate nucleus (Fig. 4b).

In Figs. 4c and d, the internal capsule, the corpus callosum, and the limbic fibers (cingulum bundle and fornix) are well visible in the fetal brain. Poor development of the external capsule is apparent. The retrolenticular part of the internal capsule and sagittal stratum is visible, but not well-established. The sagittal stratum has patches of tangential axonal fibers (green color) and a radial columnar organization (red color), suggesting that axon invasion to the radial scaffold for neural migration is underway. Superior to the internal capsule, the corona radiata is not well-developed (Fig. 4d). The superior longitudinal fasciculus is not visible in the fetus and not well-developed in the neonate either.

Assessment of major white matter tracts

Limbic fibers

Fig. 5 shows 3D reconstruction results of two important limbic fibers, the cingulum and the fornix. These are two of the most dominant tracts in the fetal brain and their entire trajectories are already developed at 19 gestational weeks.

Commissural fibers

Results of 3D reconstruction of the corpus callosum (cc) are shown in Figs. 6a–c, together with parasagittal slices (Figs. 6d–f). For fetal brain at 20 gestational weeks, formation of the cc is more advanced in the frontal lobe rather than the occipital lobe of the fetal brain. Enlargement of the genu of the cc is already appreciable. On the other hand, callosal fibers in the occipital lobe are not well-developed (outlined by the yellow dashed circle in Fig. 6a). This is also apparent in Fig. 4c, in which the forceps major (Fmajor) is much smaller than the forceps minor (Fminor) in the fetus. In the sagittal slices (Figs. 6d–f), the corpus callosum does not extend to the posterior region and the splenium is not well-developed yet. At birth, the splenium and the forceps major are quite identifiable (Figs. 4c and 6e), but the tracking results do not extend to some regions in the frontal and parietal lobe (outlined by the pink dashed circle in Fig. 6b). This is because the superior regions of the corona radiata (indicated by a pink arrow in Fig. 6h) tend to have low diffusion anisotropy (FA=0.1–0.2) in the neonate stage (Hermoye et al., 2006). This is a region where anisotropy is relatively low even in adult brains (typically FA=0.3–0.4), which is attributed to the mixture of three prominent tracts with different orientations (the corpus callosum, projection fibers, and the superior longitudinal fasciculus) (Wiegell et al., 2000; Tuch et al., 2003).

In coronal sections (Figs. 6g–i), white matter layers accounting for the callosal fibers (indicated by cyan arrows) and projection/association fibers (sagittal stratum, indicated by green arrows) are already apparent at 19 gestational weeks. This configuration is preserved in older brains, but tract structures of the later stages are clearly more convoluted (e.g. see regions indicated by pink and yellow arrowheads).

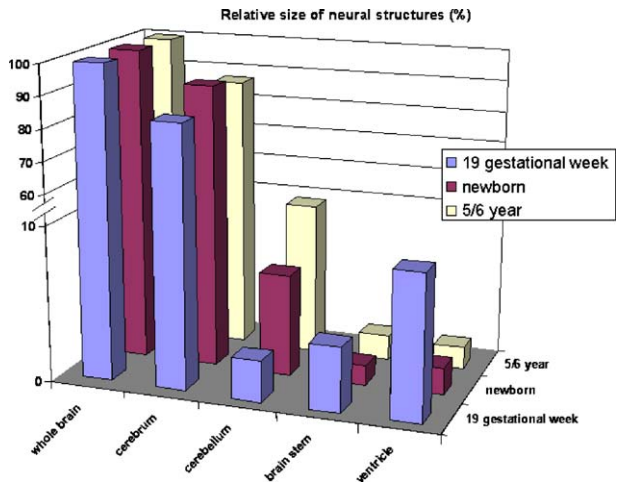

Fig. 3. Relative sizes of neural structures at 19 gestational week, 0-year and 5/6-year brains.

Association fibers

The sagittal stratum (ss) and the external capsule contain major association fibers, such as the uncinate fasciculus (unc) and the inferior fronto-occipital fasciculus (ifo)/inferior longitudinal fasciculus (ilf). Among these fibers, the unc can be clearly identified in the fetal brain (Figs. 4b, and a). The ifo and ilf, which are the major constituents of the sagittal stratum, can be identified in neonates (Fig. 7b, see also Figs. 6g–i, green arrowheads), but are not developed enough to reveal their projection to the frontal, temporal and occipital lobes by tractography (Figs. 7a–c). The coronal views (Figs. 7d–f) also show poor development of the external capsule in the fetus.

The lack of a superior longitudinal fasciculus (slf) is most striking in the fetal brain. The slf is not prominent enough, even at birth, to be reliably reconstructed by tractography (Figs. 7b and e). The temporal projection of the slf is clearly identifiable in the 5-year-old volunteer (indicated by the yellow arrow in Fig. 6i), but completely missing in the fetal brain (Fig. 6g).

Projection fibers

Major projection fibers (cortico-thalamic, thalamo-cortical, and cortical–brainstem/spinal cord connections) penetrate the corona radiata, the internal capsule, and the cerebral peduncle. The core regions of these tracts, the internal capsule and the cerebral peduncle, are well-developed in the early phase of development, although the peripheral regions (the corona radiata) are not well-visible in the fetal brain (Fig 8).

Quantitative assessment of white matter development

Sizes of various white matter tracts were obtained by manually delineating the boundary using color-coded orientation maps (Fig. 4) and measuring the cross-sectional areas. Measured white matter tracts, their locations, and results are summarized in Table 2. The quantified results confirm our qualitative observation described above. In the brainstem, the descending fibers (corticospinal,

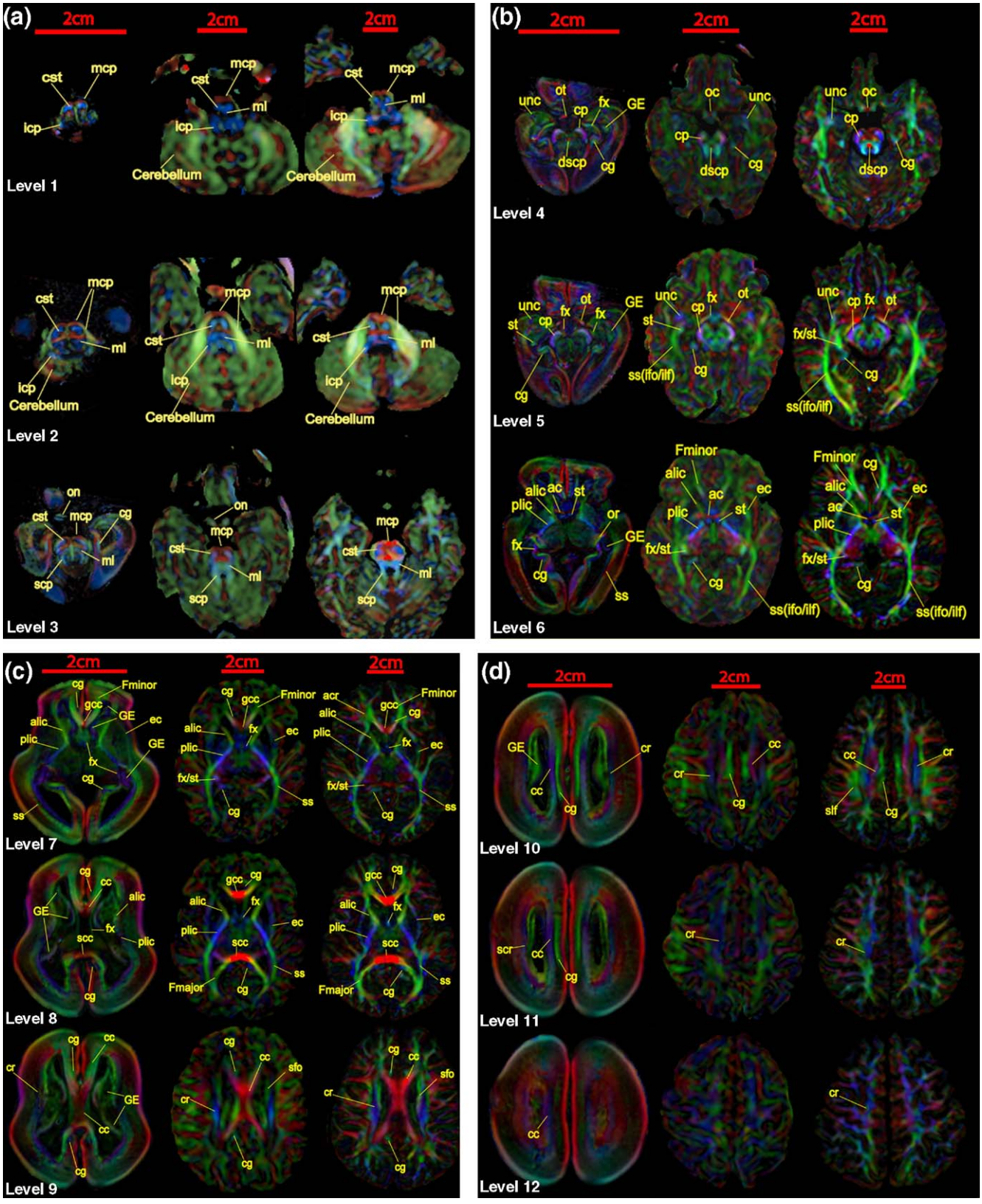

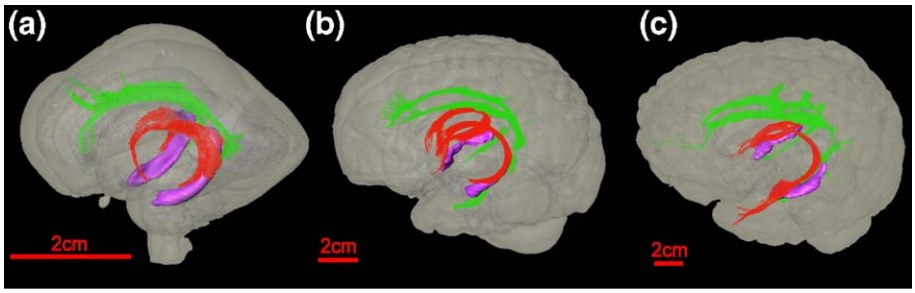

Fig. 5. 3D reconstruction of the white matter tracts of the limbic system (a: 19 gestational week fetal brain, b: 0 month old neonate brain, c: 5-year-old pediatric subject). The fornix (fx, red) and cingulum (cg, green) are reconstructed. The pink structure is the hippocampus.

corticopontine, and corticobulbar tracts) reach 16% of the size in the pediatric brain, while the middle cerebellar peduncle is only about 3%. In the midbrain, the cerebral peduncle is well-developed and contains the descending fibers. In the cerebral hemisphere, well-developed fibers include the cingulum, the uncinate fasciculus, and the anterior limb of the internal capsule. The ratios of the width of the splenium and the genu to the corpus callosum are approximately 1–1.2 for newborns and pediatric brains, while that of 19–20 gestational week fetuses is only 0.17 (the genu is larger). The proportion of the anterior and posterior limb of the internal capsule also indicates that the anterior region is more developed. It is, in general, difficult to quantify the sizes of white matter tracts and compare them between different age groups when there is a large number of anatomical differences. Corresponding anatomical locations are difficult to identify, and normalization with respect to the brain size is not straightforward. Therefore, these numbers should be used to grasp the overall trend of anatomical changes. Nonetheless, DTI allows us to perform this type of analysis, which helps to understand the order of the white matter development process.

Ganglionic eminence

The ganglionic eminence (GE) is a transient structure that can be identified only in the early phases of brain development. This structure is believed to be the precursor of the caudate, the putamen, a part of the thalamus, and the amygdala (Sidman and Rakic, 1982). The GE can be identified easily with MRI because of its unique T_1 signature (Fig. 1e). Its 3D structure and relationship with other related structures are shown in Fig. 9a. The close relationship of the GE with the caudate is clear, indicating that caudate formation is still underway at this stage. Although the GE looks homogeneous on T_1-weighted images, it is quite inhomogeneous in anisotropy and ADC maps (Figs. 1b, c, and d). Namely, it has a high FA/low ADC layer at the surface of the ventricle and a low FA/high ADC core. This high FA layer has strong orientation coherence along the ventricle surface, which allows us to reconstruct this layer by tractography, as shown in Fig. 9b. The projection of this layer resembles closely that of the stria terminalis. It is likely that this layer is a precursor of the stria terminalis that connects the amygdala and septum/hypothalamus, which are located at the two extreme ends of the GE.

Cerebral cortex

Fig. 10 shows a magnification of the early cortical formation in a fetal brain. In T_1-weighted images and FA maps, three layers can be clearly identified. The outermost layer is characterized by high intensity on T_1-weighted images and high FA, which corresponds to the cortical plate, a precursor of the cortex. The second layer is dark, both in T_1-weighted images and FA. This thick layer is the subplate, a transient structure that is not visible at later stages (Kostovic et al., 2002). The third layer demonstrates high intensity on T_1-weighted images and high FA, which should correspond to fetal white matter (intermediate zone). The fiber orientations of the first two layers are radially oriented (red color), while that of the third layer is tangential (green or blue in Fig 10e). The columnar orientation is likely due to a radial scaffold formed by radial glia and tangential fibers that grow axons. In ADC maps, the first two layers have a similar ADC, while the intermediate zone has a lower ADC. Notably, there is a narrow band with a low ADC between the cortical plate and the subplate. The neuroepithelium and the subventicular zone could not be defined clearly with MRI at this stage. Thinning of the subplate is observed in the cingulate gyrus, insula, and entorhinal cortex, as well

Fig. 4. (a) Axial images of a 19 gestational week fetal, 0-year, and 5-year brains at brainstem levels with anatomical assignment. The annotation of the structures in the fetal brains was based on available Bayer and Altman histology-based atlases (Bayer and Altman, 2004, 2005) for Figs. 3a to d. Abbreviations: ac: anterior commissure; alic: anterior limb of internal capsule; cc: corpus callosum; cc-g: genu of corpus callosum; cc-s: splenium of corpus callosum; cg: cingulum; cr: corona radiata; cst: cortical spinal tract; dscp: decussation of superior cerebellar peduncle; ec: external capsule; fmajor: forceps major; fx: fornix; gcc: genu of corpus callosum; GE: ganglionic eminence; icp: inferior cerebellar peduncle; ifo: inferior fronto-occipital peduncle; ilf: inferior longitudinal fasciculus; mcp: middle cerebellar peduncle; ml: medial lemniscus; oc: optical chiasm; on: optical nerve; or: optical radiation; ot: optical tract; plic: posterior limb of internal capsule; scc: splenium of corpus callosum; scp: superior cerebellar peduncle; scr: superior region of corona radiata; sfo: superior fronto-occipital fasciculus; ss: sagittal stratum; st: stria terminalis; and unc: uncinate fasciculus. (b) Axial images of 19 gestational week fetal, 0-year, and 5-year brains at the midbrain level with anatomical assignment. See Fig. 3a for abbreviations. (c) Axial images of 20 gestational week fetal, 0-year, and 5-year brains at the level of the corpus callosum with anatomical assignment. See Fig. 3a for abbreviations. (d) Axial images of 20 gestational week fetal, 0-year, and 5-year brains at the level of the superior corona radiata with anatomical assignment. See Fig. 3a for abbreviations.

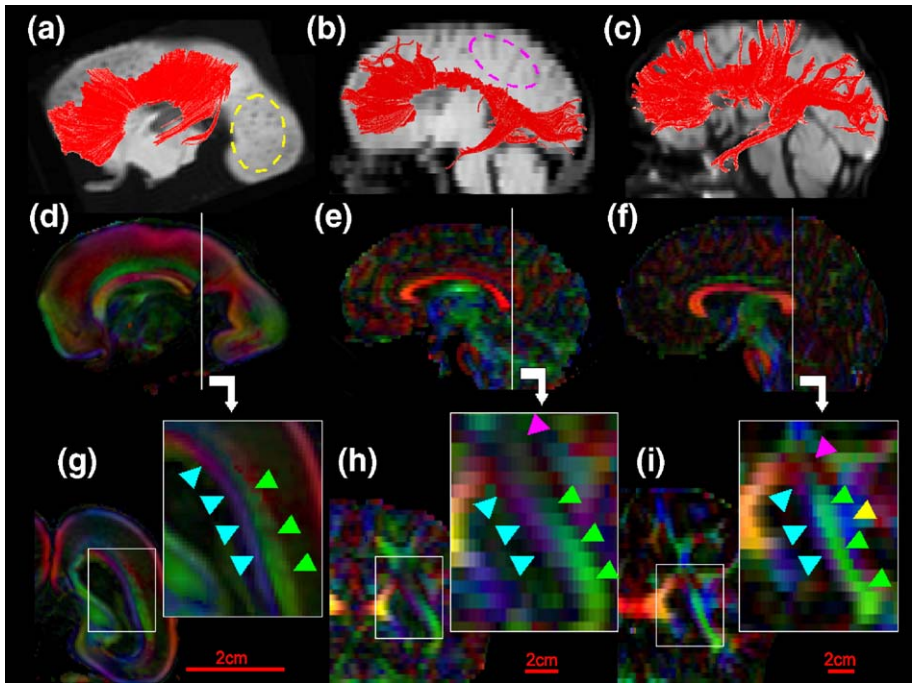

Fig. 6. Anatomy of the corpus callosum in 3D (a–c) and 2D slices (d–i). Three-dimensional tractography results are shown in panels a–c for 20 gestational week fetal brain, neonatal brain, and pediatric brain, respectively. Images in panels d–f show para-mid-sagittal slices. The corpus callosum is not well-developed in the occipital lobe in the fetus, which is apparent from 3D tracking (a, indicated by a yellow circle) and the color map (d). Coronal slices indicated by white lines in panels d–f are shown in panels g–i. White matter tracts indicated by blue arrows are commissural fibers, while those indicated by green arrows are the sagittal stratum. Pink arrows indicate regions where various families of tracts with different orientations are believed to be merged and diffusion anisotropy is low. This low anisotropy leads to lack of labeling of the corpus callosum in the area indicated by the pink circle in panel b.

as in areas where cortical folding occurs, such as the parieto-occipital sulcus, as indicated by yellow arrows in Fig 10b.

Discussion

The anatomy of fetal brains at 19–20 gestational weeks was studied by DTI and compared with neonatal and 5- to 6-year-old brains. Being sensitive to structural alignment, DTI is an excellent imaging method for delineating of the anatomy of premature brains (Huppi et al., 1998; Neil et al., 1998; Mori et al., 2001, 2005; McKinstry et al., 2002; Mukherjee et al., 2002; Maas et al., 2004; Partridge et al., 2004; Schneider et al., 2004; Hermoye et al., 2006). MRI and DTI data about the human fetus could be important resources for two future applications: (1) basic research

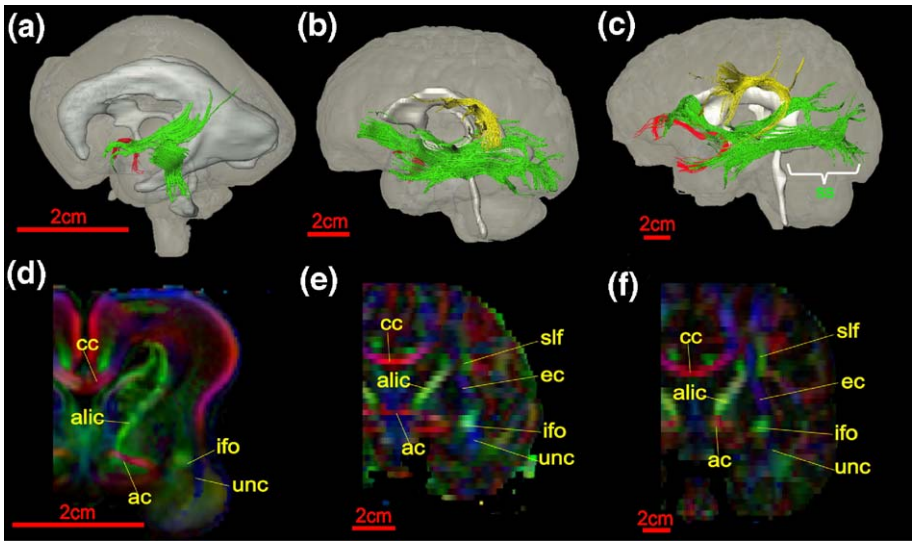

Fig. 7. Anatomy of developing association fibers in 3D reconstruction (a–c) and coronal slices (d–f) in 19 gestational week fetal, neonatal, and pediatric brains, respectively. Red, green, and yellow fibers in panels a–c are the uncinate fasciculus, the inferior fronto-occipital/inferior longitudinal fasciculus, and the superior longitudinal fasciculus. Abbreviations are the same as in Fig. 3a. White and yellow structures in panels a–c are the ventricles and the thalamus.

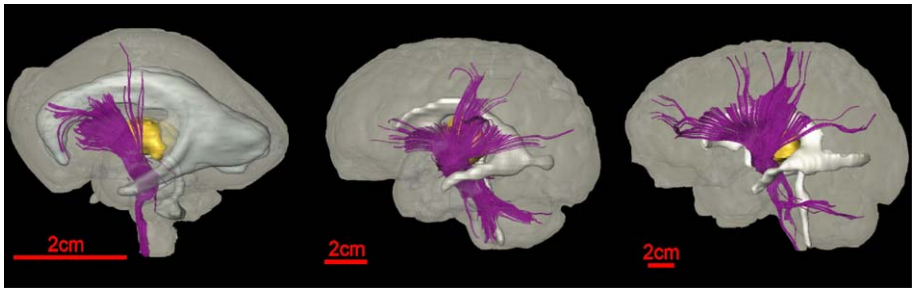

Fig. 8. 3D reconstruction of projection fibers of 19 gestational week fetal, neonatal, and pediatric brains, respectively.

in human brain development; and (2) the diagnosis of developmental brain abnormalities.

The main body of our anatomical knowledge of fetal brain development has been based on histology, but there are a surprisingly small number of resources that systematically describe the developmental processes of the human brain. Most of available atlases are based on cartoonography. Excellent resources are the recently published atlases by Bayer and Altman (2004, 2005). Although MRI-based anatomy studies cannot provide anatomic information as detailed as that provided by histology, MRI excels in characterizing the 3D architecture of the developing brain. The analysis of growing axonal bundles, in particular, is difficult to study with histology-based techniques. The use of MRI-based techniques, together with histology, could enhance our understanding of the dynamics of human brain development (Kostovic et al., 2002). Because of a small number of samples, we could characterize only the macroscopic development process in this paper and caution should be exerted in interpretation of quantitative data such as those reported in Tables 1 and 2. Nonetheless, our results clearly illustrate that DTI is a powerful tool to delineate neuroanatomy of developing human brains.

One of the important aspects of MRI-based fetal studies is the potential for future applications to clinical studies. In various brain development diseases, such as cerebral palsy, it has been reported that white matter injuries often occur in specific white matter tracts (Huppi and Inderc, 2001; Hoon et al., 2002; Miller et al., 2002; Lee et al., 2005; Thomas et al., 2005). The cause and timing of insults could be highly variable. It is not well understood how and when the injuries occur and how they progress. For example, the loss of a specific tract could represent selective degeneration of the tracts that once formed normally or could be due to inadequate or pathologic development. Characterization of the normal process of individual white matter tracts is the first step in understanding any abnormalities. In this regard, it is exciting to see that *in vivo* MRI/DTI can now be used to image neonates and premature infants in clinical settings (Maas et al., 2004; Partridge et al., 2004; Thomas et al., 2005).

Postmortem MRI studies and *in vivo* clinical DTI of premature brains have already been reported, and many of our findings in this paper have confirmed these previous findings. Kostovic et al. (2002) provided a comprehensive description of the cortical development of postmortem fetuses in the second and third trimester (15–36 gestational week) using histology and T_1-weighted images. Our observation of the subplate with T_1-weighted images agrees with their findings. *In vivo* studies (Neil et al., 1998) of infants reported high anisotropy in the cortical plate and low anisotropy in the subplate, which, again, agrees with our observation. This agreement between *in vivo* and *ex vivo* DTI is encouraging because it suggests

Table 2
White matter (WM) tract cross-sectional area normalized according to the size of a 5/6-year-old pediatric brain

WM tracts	Time point	19/20 gw	Neonate	5/6 years
Brainstem				
Midpon/axial slice level 2 (%)	cst/cpt/cbt	16.07±1.41	37.84±6.04	100.00±10.20
	ml	5.19±0.38	50.17±2.27	100.00±10.88
	mcp	2.81±0.39	30.15±3.09	100.00±10.88
	icp	5.02±0.74	61.86±6.22	100.00±14.02
Midbrain				
Lower midbrain/axial slice level 3 (%)	scp	5.46±0.83	40.97±3.83	100.00±5.66
Middle midbrain/axial slice level 4 (%)	cp	15.46±0.80	64.48±3.83	100.00±5.66
Cerebrum				
Mid-sagittal slice	cc (%)	4.72±0.52	48.85±3.21	100.00±11.65
	cc-s/cc-g	0.17±0.02	1.15±0.08	0.99±0.08
Middle midbrain/axial slice level 4 (%)	cg	10.13±0.78	63.17±8.90	100.00±13.26
	unc	8.27±0.31	64.92±9.67	100.00±14.80
Lower hemisphere/axial slice level 6 (%)	ss	4.67±0.51	44.67±6.54	100.00±3.67
Middle hemisphere/axial slice level 7 (%)	alic	8.46±0.94	57.99±3.09	100.00±15.23
	plic	4.86±0.65	46.27±4.11	100.00±15.55
Upper hemisphere/axial slice level 9 (%)	scr	5.34±0.77	43.26±6.75	100.00±11.98
Upper hemisphere/axial slice level 10 (%)	slf	0.00±0.00	19.01±2.49	100.00±6.53

Standard deviations are calculated from 3 samples at each time point. The measured regions are also indicated in Fig. 4. The slice level is in accordance with that in Fig. 4. Abbreviations are listed in Fig. 4a. Ratios of the width of the genu (cc-g) and splenium (cc-s) of the corpus callosum are also calculated at the mid-sagittal plane.

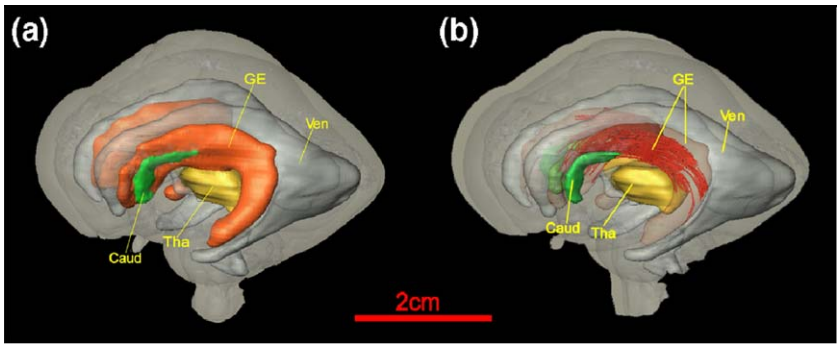

Fig. 9. 3D reconstruction of the ganglionic eminence (GE, orange) of a 19 gestational week fetal brain (a) and fibrous structures (red) running along the GE, demonstrated by tractography (b). White, green, and yellow structures are the ventricles (Ven), caudate (Caud), and thalamus (Tha).

that the postmortem DTI essentially carries anatomical information analogous to that reported from *in vivo* studies. Because most *in vivo* neonate DTI is limited in scanning time and spatial resolution, our high-resolution images have value as an anatomical reference for *in vivo* studies. On the other hand, it is also important to note that some postmortem samples are not well-preserved and, in severe cases, diffusion anisotropy is lost or there is an extremely short T_2. At this moment, we do not have an established method to quantify the quality of sample preservation and it is likely that each sample has a different degree of preservation quality. Therefore, postmortem-based studies could be used as a morphological description of anatomy, providing information such as shape, thickness, location, and trajectory, but these studies are probably not reliable for quantification of contrasts such as absolute T_2, T_1, FA, and ADC values. Our primary focus in this study was the white matter anatomy of the fetus because existing knowledge about the white matter is scarce and DTI is an excellent tool for identification of the tracts. Tractography played an important role in the assignment of the tracts annotated in Fig. 4. Callosal fibers are among the most studied white matter tracts, probably due to easy identification at the mid-sagittal level. As reported previously (Kier and Truwit, 1996), the anterior commissure and the corpus callosum are already formed at 19–20 gestational weeks. In general, white matter formation progresses from the core to the periphery and from the anterior to the posterior regions of the brain.

Early formation of the limbic system is well known, and it is expected that limbic fibers are well formed at 19–20 gestational weeks (Bayer and Altman, 2005). Poorly developed tracts include peripheral (subcortical) white matter and association fibers at the external capsule and sagittal stratum. The slf is not detectable in the fetal brain with the current image resolution. This hierarchical order of tract formation agrees well with a report by Partridge et al. (2004), in which order of maturation process was studied by FA and ADC measurements at postnatal stages.

We have also described cortical formation. Both T_1-weighed images and DTI can clearly identify the cortical plate, subplate, and

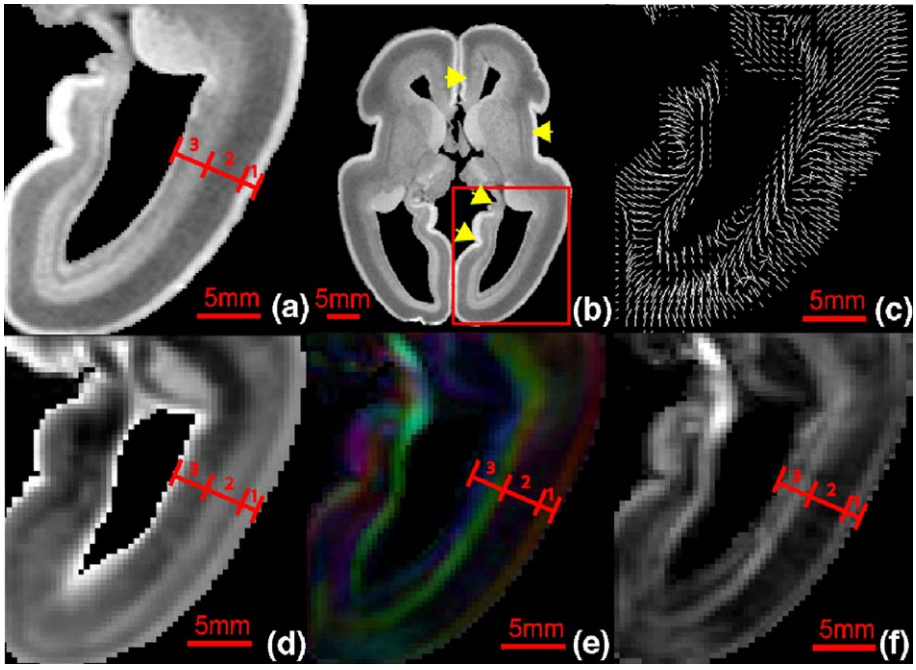

Fig. 10. Detailed anatomy of the cortex of a 20 gestational week fetal brain on a T_1-weighted image (a), vector map (c), ADC map (d), DT color map (e), and FA map (f). (b) is the axial slice of T_1-weighted image showing the location where the enlargement takes place. Yellow arrows indicate the areas where the subplate becomes thinner. Layers 1, 2, and 3 are the cortical plate, the subplate, and the intermediate zone, respectively.

intermediate zone (white matter). The subplate is a transient structure important for neural migration and axonal guidance. This structure has already been described in premature infants using *in vivo* DTI (Maas et al., 2004). We observed high ADC in the subplate, which agrees with the finding by Maas et al., but the high ADC we have observed in the cortical plate is not in agreement. This is most likely due to difference in gestational age (19–20 weeks vs. 25–27 weeks), but possibility of fixation artifacts cannot be excluded. Between the cortical plate and subplate, there is a narrow band with low ADC. The assignment of this structure is not clear at this point. There is a radial arrangement of structures in the cortical plate and subplate, as previously reported in human and mice (Thornton et al., 1997; Neil et al., 1998; Mori et al., 2001; McKinstry et al., 2002). The axonal architecture of the intermediate zone could be clearly delineated by color maps. In some regions, radial and tangential orientations are mixed, indicating transition from a radial organization to axon-rich white matter.

It has been postulated that injuries of specific white matter tracts in cerebral palsy are due to an incomplete state of development of the vascular supply to the cerebral white matter and the maturation-dependent vulnerability of the oligodendroglia precursor cells (the timing of insults and actively growing of axons) (Huppi et al., 1998; Barkovich, 2000; Volpe, 2001; Neil et al., 2002). From histology-based studies, Haynes et al. found that the parietal white matter is actively growing in perinatal period and hypothesized that they are susceptible to PVL (Haynes et al., 2005). Thus, mapping of white matter development could provide important clues to understanding the mechanism of selective white matter injuries. Our previous DTI study of periventricular leukomalacia (PVL) patients revealed that limbic fibers are well-preserved, while posterior regions of the corpus callosum, corona radiata, and sagittal stratum are most severely affected (Hoon et al., 2002). This observation agrees with the pattern of white matter formation of the fetuses. Namely, these affected tracts are being formed in the perinatal period when the insult occurred, while the limbic fibers have already been formed. This also implies that the massive loss of the white matter in PVL patients is not due to the degeneration of previously formed white matter tracts, but, rather, due to the lack of formation of the tracts. One possible implication of this hypothesis is that severe perinatal injuries could be well-visualized by DTI at birth when most of white matter tracts are supposed to be already established in normal full-term subjects. Delineation of these specific white matter tracts has not been possible with conventional MRI. DTI may make it possible to detect white matter injuries in specific tracts much earlier than with conventional image-based diagnosis. However, this is a hypothesis that remains to be tested.

Conclusion

DTI provides high contrast that enables differentiation of white matter structures in immature brains. Various neural structures in 19- and 20-gestational week fetal brains were assigned, annotated, and evaluated three-dimensionally. The fetal anatomy was compared with 0-month neonates and 5-year-old subjects. Varying degrees of the maturation status of fibers in the brainstem, projection, association, and commissural fibers were delineated. Most white matter tracts have already formed at 0 month. These data could be a valuable anatomical reference for clinical pediatric diagnosis as well as for basic human development studies.

Acknowledgments

This work was supported by NIH grants EB003543, AG20012, RR15241, and NS045841. Dr. van Zijl is a paid lecturer for Philips Medical Systems. This arrangement has been approved by Johns Hopkins University in accordance with its conflict of interest policies.

References

Barkovich, A.J., 2000. Pediatric Neuroimaging. Lippincott Wiliams and Wilkins, Philadelphia.

Basser, P.J., Mattiello, J., Le Bihan, D., 1994. MR diffusion tensor spectroscopy and imaging. Biophys. J. 66, 259–267.

Bayer, S.A., Altman, J., 2004. The Human Brain During the Third Trimester. CRC Press.

Bayer, S.A., Altman, J., 2005. The Human Brain During the Second Trimester. CRC Press.

Catani, M., Howard, R.J., Pajevic, S., Jones, D.K., 2002. Virtual in vivo interactive dissection of white matter fasciculi in the human brain. NeuroImage 17, 77–94.

Haynes, R.L., Borenstein, N.S., Desilva, T.M., Folkerth, R.D., Liu, L.G., Volpe, J.J., Kinney, H.C., 2005. Axonal development in the cerebral white matter of the human fetus and infant. J. Comp. Neurol. 484, 156–167.

Hermoye, L., Saint-Martin, C., Cosnard, G., Lee, S.K., Kim, J., Nassogne, M.C., Menten, R., Clapuyt, P., Donohue, P.K., Hua, K., Wakana, S., Jiang, H., van Zijl, P.C.M., Mori, S., 2006. Pediatric diffusion tensor imaging: normal database and observation of the white matter maturation in early childhood. NeuroImage 29, 493–504.

Hoon Jr., A.H., Lawrie Jr., W.T., Melhem, E.R., Reinhardt, E.M., van Zijl, P.C.M., Solaiyappan, M., Jiang, H., Johnston, M.V., Mori, S., 2002. Diffusion tensor imaging of periventricular leukomalacia shows affected sensory cortex white matter pathways. Neurology 59, 752–756.

Huppi, P.S., Inderc, T.E., 2001. Magnetic resonance techniques in the evaluation of the perinatal brain: recent advances and future directions. Semin. Neonatol. 6, 195–210.

Huppi, P., Maier, S., Peled, S., Zientara, G.P., Barnes, P.D., Jolesz, F.A., Volpe, J.J., 1998. Microstructural development of human newborn cerebral white matter assessed in vivo by diffusion tensor magnetic resonance imaging. Pediatr. Res. 44, 584–590.

Jones, D.K., Horsfield, M.A., Simmons, A., 1999. Optimal strategies for measuring diffusion in anisotropic systems by magnetic resonance imaging. Magn. Reson. Med. 42, 515–525.

Kier, E.L., Truwit, C.L., 1996. The normal and abnormal genu of the corpus callosum: an evolutionary, embryologic, anatomic, and MR analysis. Am. J. Neuroradiol. 17, 1631–1641.

Kostovic, I., Judas, M., Rados, M., Hrabac, P., 2002. Laminar organization of the human fetal cerebrum revealed by histochemical markers and magnetic resonance imaging. Cereb. Cortex 12, 536–544.

Lee, S.K., Kim, D.I., Kim, J., Kin, D.J., Kim, H.D., Kim, D.S., Mori, S., 2005. Diffusion-tensor MR imaging and fiber tractography: a new method of describing aberrant fiber connections in developmental CNS anomalies. Radiographics 25, 53–65 (discussion 66-58).

Maas, L.C., Mukherjee, P., Carballido-Gamio, J., Veeraraghavan, S., Miller, S.P., Partridge, S.C., Henry, R.G., Barkovich, A.J., Vigneron, D.B, 2004. Early laminar organization of the human cerebrum demonstrated with diffusion tensor imaging in extremely premature infants. NeuroImage 22, 1134–1140.

Makris, N., Worth, A.J., Sorensen, A.G., Papadimitriou, G.M., Reese, T.G., Wedeen, V.J., Davis, T.L., Stakes, J.W., Caviness, V.S., Kaplan, E., Rosen, B.R., Pandya, D.N., Kennedy, D.N., 1997. Morphometry of in vivo human white matter association pathways with diffusion weighted magnetic resonance imaging. Ann. Neurol. 42, 951–962.

McKinstry, R.C., Mathur, A., Miller, J.H., Ozcan, A., Snyder, A.Z., Schefft,

G.L., Almli, C.R., Shiran, S.I., Conturo, T.E., Neil, J.J., 2002. Radial organization of developing preterm human cerebral cortex revealed by non-invasive water diffusion anisotropy MRI. Cereb. Cortex 12, 1237–1243.

Miller, S.P., Vigneron, D.B., Henry, R.G., Bohland, M.A., Ceppi-Cozzio, C., Hoffman, C., Newton, N., Partridge, J.C., Ferriero, D.M., Barkovich, A.J., 2002. Serial quantitative diffusion tensor MRI of the premature brain: development in newborns with and without injury. J. Magn. Reson. Imaging 16, 621–632.

Mori, S., Crain, B.J., Chacko, V.P., van Zijl, P.C.M., 1999. Three dimensional tracking of axonal projections in the brain by magnetic resonance imaging. Ann. Neurol. 45, 265–269.

Mori, S., Itoh, R., Zhang, J., Kaufmann, W.E., van Zijl, P.C.M., Solaiyappan, M., Yarowsky, P., 2001. Diffusion tensor imaging of the developing mouse brain. Magn. Reson. Med. 46, 18–23.

Mori, S., Wakana, S., Nagae-Poetscher, L.M., van Zijl, P.C.M., 2005. MRI Atlas of Human White Matter. Elsevier, Amsterdam.

Mukherjee, P., Miller, J.H., Shimony, J.S., Philip, J.V., Nehra, D., Snyder, A.Z., Conturo, T.E., Neil, J.J., McKinstry, R.C., 2002. Diffusion-tensor MR imaging of gray and white matter development during normal human brain maturation. AJNR Am. J. Neuroradiol. 23, 1445–1456.

Neil, J.J., Shiran, S., McKinstry, R., Schefft, G.L., Snyder, A.Z., Almli, C.R., Akbudak, E., Arnovitz, J.A., Miller, J.P., Lee, B.C., Conturo, T.E., 1998. Normal brain in human newborns: apparent diffusion coefficient and diffusion anisotropy measured by using diffusion tensor MR imaging. Radiology 209, 57–66.

Neil, J.J., Miller, J., Mukherjee, P., Huppi, P.S., 2002. Diffusion tensor imaging of normal and injured developing human brain—A technical review. NMR Biomed. 15, 543–552.

Partridge, S.C., Mukherjee, P., Henry, R.G., Miller, S.P., Berman, J.I., Jin, H., Lu, Y., Glenn, O.A., Ferriero, D.M., Barkovich, A.J., Vigneron, D.B., 2004. Diffusion tensor imaging: serial quantitation of white matter tract maturity in premature newborns. NeuroImage 22, 1302–1314.

Pierpaoli, C., Basser, P.J., 1996. Toward a quantitative assessment of diffusion anisotropy. Magn. Reson. Med. 36, 893–906.

Schneider, J.F., Il'yasov, K.A., Hennig, J., Martin, E., 2004. Fast quantitative diffusion-tensor imaging of cerebral white matter from the neonatal period to adolescence. Neuroradiology 46, 258–266.

Sidman, R.L., Rakic, P., 1982. Development of the human central nervous system. In: Haymaker, W., Adams, R.D. (Eds.), Histology and Histopathology of the Nervous System. Thoms, Springfield, IL, pp. 3–145.

Stieltjes, B., Kaufmann, W.E., van Zijl, P.C.M., Fredericksen, K., Pearlson, G.D., Mori, S., 2001. Diffusion tensor imaging and axonal tracking in the human brainstem. NeuroImage 14, 723–735.

Thomas, B., Eyssen, M., Peeters, R., Molenaers, G., Van Hecke, P., De Cock, P., Sunaert, S., 2005. Quantitative diffusion tensor imaging in cerebral palsy due to periventricular white matter injury. Brain 128, 2562–2577.

Thornton, J.S., Ordidge, R.J., Penrice, J., Cady, E.B., Amess, P.N., Punwani, S., Clemence, M., Wyatt, J.S., 1997. Anisotropic water diffusion in white and gray matter on the neonatal piglet brain before and after transient hypoxia–ischaemia. Magn. Reson. Imaging 15, 433–440.

Tuch, D.S., Reese, T.G., Wiegell, M.R., Wedeen, V.J., 2003. Diffusion MRI of complex neural architecture. Neuron 40, 885–895.

Volpe, J.J., 2001. Neurobiology of periventricular leukomalacia in the premature infant. Pediatr. Res. 50, 553–562.

Wakana, S., Jiang, H., Nagae-Poetscher, L.M., van Zijl, P.C.M., Mori, S., 2004. Fiber tract-based atlas of human white matter anatomy. Radiology 230, 77–87.

Wiegell, M., Larsson, H., Wedeen, V., 2000. Fiber crossing in human brain depicted with diffusion tensor MR imaging. Radiology 217, 897–903.

Xue, R., van Zijl, P.C.M., Crain, B.J., Solaiyanppan, M., Mori, S., 1999. In vivo three-dimensional reconstruction of rat brain axonal projections by diffusion tensor imaging. Magn. Reson. Med. 42, 1123–1127.